

## Cantharidin decreased viable cell number in human osteosarcoma U-2 OS cells through G<sub>2</sub>/M phase arrest and induction of cell apoptosis

Chia-Ching Chen<sup>a</sup>, Fu-Shin Chueh<sup>b</sup>, Shu-Fen Peng<sup>a</sup>, Wen-Wen Huang<sup>a</sup>, Chang-Hai Tsai<sup>c,d</sup>, Fuu-Jen Tsai<sup>d,e</sup>, Chih-Yang Huang<sup>f,g,h,i,j,k,l</sup>, Chih-Hsin Tang<sup>h,i,l</sup>, Jai-Sing Yang<sup>j</sup>, Yuan-Man Hsu<sup>l</sup>, Mei-Chin Yin<sup>b,j</sup>, Yi-Ping Huang<sup>k</sup> and Jing-Gung Chung<sup>a,l</sup>

<sup>a</sup>Department of Biological Science and Technology, China Medical University, Taichung, Taiwan; <sup>b</sup>Department of Food Nutrition and Health Biotechnology, Asia University, Taichung, Taiwan; <sup>c</sup>China Medical University Children's Hospital, China Medical University, Taichung, Taiwan; <sup>d</sup>Department of Healthcare Administration, Asia University, Taichung, Taiwan; <sup>e</sup>School of Chinese Medicine, College of Chinese Medicine, China Medical University, Taichung, Taiwan; <sup>f</sup>Graduate Institute of Biomedical Sciences, China Medical University, Taichung, Taiwan; <sup>g</sup>Graduate Institute of Chinese Medical Science, China Medical University, Taichung, Taiwan; <sup>h</sup>Chinese Medicine Research Center, China Medical University, Taichung, Taiwan; <sup>i</sup>Department of Pharmacology, School of Medicine, China Medical University, Taichung, Taiwan; <sup>j</sup>Department of Medical Research, China Medical University Hospital, China Medical University, Taichung, Taiwan; <sup>k</sup>Department of Physiology, College of Medicine, China Medical University, Taichung, Taiwan; <sup>l</sup>Department of Biotechnology, College of Medical and Health Science, Asia University, Taichung, Taiwan

### ABSTRACT

Cantharidin (CTD), a sesquiterpenoid bioactive substance, has been reported to exhibit anticancer activity against various types of cancer cells. The aim of the present study was to investigate the apoptosis effects and the underlying mechanisms of CTD on osteosarcoma U-2 OS cells. Results showed that CTD induced cell morphologic changes, reduced total viable cells, induced DNA damage, and G<sub>2</sub>/M phase arrest. CTD increased the production of reactive oxygen species and Ca<sup>2+</sup>, and elevated the activities of caspase-3 and -9, but decreased the level of mitochondrial membrane potential. Furthermore, CTD increased the ROS- and ER stress-associated protein expressions and increased the levels of pro-apoptosis-associated proteins, but decreased that of anti-apoptosis-associated proteins. Based on these observations, we suggested that CTD decreased cell number through G<sub>2</sub>/M phase arrest and the induction of cell apoptosis in U-2 OS cells and CTD could be a potential candidate for osteosarcoma treatments.

### ARTICLE HISTORY

Received 12 March 2019  
Accepted 22 May 2019

### KEYWORDS

Cantharidin; cell cycle; G<sub>2</sub>/M phase arrest; apoptosis; osteosarcoma U-2 OS cells

Osteosarcoma, the most frequent and prevalent aggressive pediatric malignancy of bone tumor, develops from mesenchymal stem cells *via* endochondral ossification which is pathologically characterized by spindle cells and aberrant osteoid formation [1,2], and it occurs higher incidence in children and adolescents [2–4]. Patients with osteosarcoma which do not have distant metastases will have a longer survival rate, but patients with metastatic or recurrent disease will reveal a lower survival rate [5]. However, if osteosarcoma caused pulmonary metastasis, the 3–5-year survival rate is about 5–20% [6,7]. Currently, the treatments of osteosarcoma including surgery, radiotherapy, and multiagent chemotherapy have an improvement in patient survival rate. However, the overall survival of patients with osteosarcoma remains unsatisfied [3,4,8,9]. Thus, to find agents from natural products are needed for treating patients with osteosarcoma.

Major pathways of apoptosis are the death receptor-mediated pathway and the mitochondria-dependent pathway [10,11]. The death receptor-mediated pathway involves in the interaction of Fas-Fas ligand to activate

caspase-8 for either directly activating caspase-3 to induce apoptosis [12,13] or affecting Bid to lead to the mitochondria-dependent pathway which involved the mitochondria membrane potential to release cytochrome c and the activations of PARP and caspase-3 for inducing apoptosis [11,14] or releases of AIF and Endo G for entering to nuclei for causing cell apoptosis [15,16]. Alternatively, *via* endoplasmic reticulum (ER) stress initiates apoptotic signals [17,18]. Thus, the strategy for anticancer drug is to induce cancer cell apoptosis through one of the apoptosis pathways.

Numerous evidences have indicated that natural products have formed an important part of drug discovery. Cantharidin (CTD), a sesquiterpenoid bioactive substance and obtained from Spanish fly or blister beetle (*Mylabris phalerata* Pall. and *Mylabris cichorii* Linn.), has been shown to present biological activities including anticancer [19]. CTD has also been shown to reduce total viable cells of many human cancer cell lines *in vitro* that through cell cycle arrest and induction of cell apoptosis [20–24]. Recently, in our laboratory, we also found that CTD significantly inhibited the growth

of human skin cancer (epidermoid carcinoma) A431 cell xenograft tumors in mice [25] and inhibited cell migration and invasion of human lung cancer NCI-H460 cells *via* uPA and MAPK signaling pathways [26].

CTD induces cytotoxic effects through the cell cycle arrest and apoptotic cell death in many human cancer cell lines, however, CTD decreased total viable cells of U-2 OS *in vitro* is still unclear. We investigated the effects of CTD on cell viability of U-2 OS *in vitro* and results indicated that CTD induced G<sub>2</sub>/M phase arrest and apoptotic cell death *via* ER stress and mitochondria-dependent pathways.

## Methods

### Test chemicals, reagents, and culture medium

Cantharidin (CTD), 4',6-Diamidino-2-Phenylindole, Dilactate (DAPI), dimethyl sulfoxide (DMSO), propidium iodide (PI) and trypsin-EDTA were obtained from Sigma-Aldrich Chemical Co. (St. Louis, MO, USA). McCoy's 5A medium, fetal bovine serum (FBS), L-glutamine and penicillin-streptomycin were purchased from GIBCO®/Invitrogen Life Technologies (Carlsbad, CA, USA). Primary antibodies against DNA damage-associated proteins (p-ATM, p-ATR, -DNA-PKcs, and PARP) and against ER stress-associated protein (caspase-4, IRE1- $\alpha$ , GADD153, and GRP78) were obtained from Cell Signaling Technology, Inc. (Beverly, MA, USA). Primary antibodies against cell cycle-associated proteins (CHK1, CDC25C, CDK1, p21, p-p53, and WEE-1) were purchased from Santa Cruz Biotechnology, Inc. (Dallas, TX, USA). Primary antibody against ROS- and apoptosis-associated proteins and internal control (SOD (Cu/Zn), SOD (Mn), catalase, caspase-3, XIAP, cytochrome c, caspase-9, Bad, Bax, Bak, Bid, Endo G, AIF, and  $\beta$ -actin) were obtained from Sigma-Aldrich (St. Louis, MO, USA). Phosphate buffered saline (PBS) and all other reagents were of analytical grade.

### Cell line and culture

Human osteosarcoma U-2 OS cells were obtained from the Food Industry Research and Development Institute (Hsinchu, Taiwan). Cells were cultured in McCoy's 5A medium supplemented 2 mM L-glutamine, 10% FBS, and penicillin-streptomycin (100 Units/mL penicillin and 100  $\mu$ g/mL streptomycin) onto 75 cm<sup>2</sup> tissue culture flasks and grown in a humidified incubator with 5% CO<sub>2</sub> at 37°C [27].

### Cell's morphological changes and percentage of cell viability assays

U-2 OS cells ( $1 \times 10^5$  cells/well) were maintained in 12-well plates with McCoy's 5A medium containing 10% FBS for 24 h and were incubated with CTD at 0,

2, 4, 6 and 8  $\mu$ M for 48 h. Cells were examined and photographed under phase contrast microscopy at 200x, and then were harvested and stained with PI (5  $\mu$ g/mL) for measuring the total viability by flow cytometry (BD Biosciences, FACSCalibur, San Jose, CA, USA) as previously described [27].

### DAPI and TUNEL staining for apoptosis

U-2 OS cells ( $1 \times 10^5$  cells/well) were cultured onto 12-well plate and incubated with CTD (0, 2, 4, 6 and 8  $\mu$ M) for 48 h. Cells were fixed in 3% paraformaldehyde for 20 min and were stained with DAPI solution (2  $\mu$ g/mL), followed by photographed using a fluorescence microscope as described previously [27]. Or cells were stained with TUNEL assay kit according to the instruction (Apo-BrdU *In Situ* DNA Fragmentation Assay Kit; Biovision, San Francisco, CA, USA) as previously described [28]. Briefly, cells were cultured at 12 well plates overnight, treated with CTD (0, 2, 4, 6 and 8  $\mu$ M) for 48 h. After incubation, cells were fixed with 1% paraformaldehyde for 15 min and permeabilized by ice-cold 70% ethanol overnight. Then, the cells were resuspended in Wash Buffer twice and then in DNA Labeling Solution (TdT reaction buffer, TdT Enzyme, and Br-dUTP) for 60 min at 37°C. Cells were rinsed with Rinse Buffer and centrifuged to remove the supernatant. Cells were resuspended in Antibody Solution containing anti-BrdU-FITC antibody in the dark for 30 min at room temperature. Moreover, then cells were treated with PI/RNase A solution and incubated in the dark for 30 min at room temperature. Finally, cells were analyzed by flow cytometry. Cells with TUNEL signals gated by M1 region were scored as TUNEL positive cells.

### PI staining for cell cycle assay and Annexin V/PI staining for apoptotic cell death assay

U-2 OS cells ( $1 \times 10^5$  cells/well) were cultured in 12-well plate and then were incubated with 0, 2, 4, 6 and 8  $\mu$ M of CTD for 48 h. Cells were isolated, incubated with 10  $\mu$ g/mL RNase A, stained with 2  $\mu$ g/mL PI, and then were analyzed by flow cytometry as described previously [28]. Or cells were incubated with 6  $\mu$ M of CTD for 0, 6, 12, 24 and 48 h. After incubation, cells were harvested and resuspended in Annexin V binding buffer, followed by incubation with Annexin V-FITC/PI in the dark for 15 min for total apoptotic cell death analysis by flow cytometry as previously described [28].

### Measurements of reactive oxygen species (ROS), intracellular Ca<sup>2+</sup>, mitochondrial membrane potential ( $\Delta\psi_m$ ), and caspase activities

Flow cytometric assay was used to measure the levels of ROS, Ca<sup>2+</sup>,  $\Delta\psi_m$  and activities of caspase-3 and caspase-9 in U-2 OS cells. In brief, cells ( $1 \times 10^5$  cells/well) in

12-well plate were incubated with 6  $\mu\text{M}$  of CTD for 0, 6, 12, 24 and 48 h. Cells were isolated and re-suspended in 500  $\mu\text{L}$  of  $\text{H}_2\text{DCF-DA}$  (10  $\mu\text{M}$ ) for ROS ( $\text{H}_2\text{O}_2$ ) measurement, in Fluo-3/AM (2.5  $\mu\text{g/mL}$ ) for intracellular  $\text{Ca}^{2+}$  concentrations measurement, and in 500  $\mu\text{L}$  of DiOC<sub>6</sub> (4  $\mu\text{mol/L}$ ) for the levels of  $\Delta\Psi_{\text{m}}$  measurement. All samples were maintained in the dark for 30 min and were analyzed by flow cytometry as described previously [28,29]. For caspase activity assay, cells were re-suspended in 25  $\mu\text{L}$  of 10  $\mu\text{M}$  substrate solution (PhiPhiLux-G<sub>1</sub>D<sub>1</sub> and CaspaLux 9-M<sub>1</sub>D<sub>2</sub> for caspase-3 and caspase-9, respectively) (OncoImmunin, Inc. Gaithersburg, MD, USA) before being incubated for 60 min at 37 °C and were analyzed activities of caspase-3 and caspase-9 by flow cytometry as described previously [28].

### **Western blotting analysis for cell cycle and apoptosis-associated proteins**

U-2 OS cells ( $1 \times 10^6$  cells/dish) were cultured onto 10-cm dishes for 24 h and were incubated with 6  $\mu\text{M}$  of CTD for 0, 6, 12, 24 and 48 h. Cells were collected, lysed, quantitated total proteins with Bio-Rad protein assay kit (Hercules, CA, USA) [27,28]. Proteins from each sample (20  $\mu\text{g}$ ) were separated by 12% (v/v) SDS-PAGE gel, and the gel were transferred onto polyvinylidene difluoride (PVDF) membranes (Millipore, Belford, MA, USA) and then the membrane was blocked with 5% skim milk powder at 37°C for 2 h. The membranes were probed with the primary antibodies against cell cycle and apoptosis-associated proteins. After washed with PBST for 45 min, the membrane was probed with peroxidase-conjugated anti-mouse IgG (Santa Cruz Biotechnology, Inc.; Dallas, TX, USA) at room temperature (25°C) for 2 h. Immunoreactive bands (protein bands) were visualized by chemiluminescence ECL detection (Bio-Rad Laboratories, Inc.; Hercules, CA, USA) [28,30].

### **Statistical analysis**

The statistical differences between control and CTD treated groups were analyzed by one-way ANOVA analysis. All experiments were performed at least 3 times. The results were expressed as the mean  $\pm$  standard deviation (SD). Significance was placed at \* $p < 0.05$ , \*\* $p < 0.01$  and \*\*\* $p < 0.001$ .

## **Results**

### **CTD induced cell morphological changes and decreased total viability in U-2 OS cells**

After cells were incubated with CTD (0, 2, 4, 6 and 8  $\mu\text{M}$ ) for 48 h, U-2 OS cells were examined and photographed and the percentage of viable cells was measured. As shown in Figure 1(a), CTD induced cell

morphological changes such as increased cell debris and the presence of detachment and shrunken cells. The viable cell number was quantified by flow cytometry and results revealed that CTD treatment significantly decreased cell viability of U-2 OS cells in a dose-dependent manner (Figure 1(b)). Statistically significant cytotoxic effects were observed in U-2 OS cells after treatment with 2, 4, 6 and 8  $\mu\text{M}$  CTD with an IC<sub>50</sub> value of 6  $\mu\text{M}$  at 48 h. Therefore, we selected 6  $\mu\text{M}$  for further experiments.

### **CTD induced chromatin condensation and DNA damage in U-2 OS cells**

U-2 OS cells were treated with CTD (0, 2, 4, 6 and 8  $\mu\text{M}$ ) for 48 h, cells were stained with DAPI and were examined and photographed by using fluorescence microscopy and results are present in Figure 2. After CTD treatment at 2–8  $\mu\text{M}$  for 48 h, cells were stained with DAPI and have brighter fluorescence in the nucleus when compared to untreated (control) cells (Figure 2(a)). Bright fluorescence of DAPI staining indicated the nicked DNA and chromatin condensation, and these effects showed in a dose-dependent manner (Figure 2(a)). TUNEL assay was also used to evaluate DNA damage by flow cytometry and results are shown in Figure 2(b). Cells treated with CTD at 4, 6, and 8  $\mu\text{M}$  for 48 h revealed significantly increased percentage of BrdU-FITC cells when compared to untreated (control) cells, indicating CTD induced DNA damage in U-2 OS cells.

### **CTD induced cell cycle arrest and cell apoptosis in U-2 OS cells**

Cells were harvested and stained by PI for cell cycle distribution assay and were double stained with Annexin-V/PI for measuring apoptotic cell death by flow cytometric assay and results are present in Figure 3. Results indicated that CTD induced G<sub>2</sub>/M phase arrest and sub-G<sub>1</sub> phase (apoptosis) but decreased G<sub>0</sub>/G<sub>1</sub> phase in U-2 OS cells (Figure 3(a)). In order to further confirm CTD induced cell apoptosis, Annexin-V/PI were used for examining apoptotic cell death and results indicated that CTD induced early and late apoptosis in U-2 OS cells and these effects are a time-dependent manner (Figure 3(b)).

### **CTD induced reactive oxygen species (ROS) and $\text{Ca}^{2+}$ productions, decreased the levels of mitochondrial membrane potential ( $\Delta\Psi_{\text{m}}$ ) and increased caspase activity in U-2 OS cells**

U-2 OS cells were incubated with CTD (0 and 6  $\mu\text{M}$ ) for 6, 12, 24 and 48 h and were harvested for

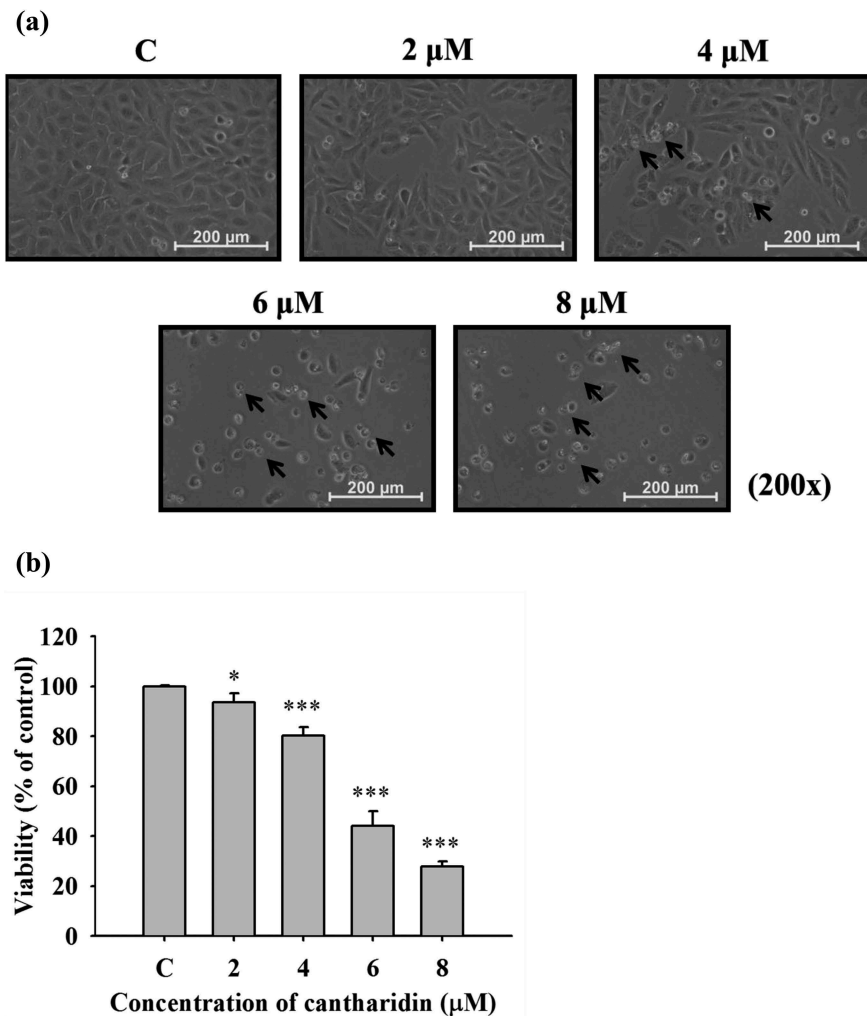


**Figure 1.** CTD induced cell morphological changes and decreased total viability of U-2 OS cells.

Cells were treated with (2, 4, 6 and 8 μM) for 48 h, cells were examined, photographed and percentage viable cells were measured (a): cell morphology; (b): total viable cells as described in Materials and Methods. The results were expressed as the mean  $\pm$  standard deviation (SD). \* $p < 0.05$ , \*\* $p < 0.01$  and \*\*\* $p < 0.001$ , significant difference between CTD-treated groups and the control as analyzed by one-way ANOVA. Arrows indicated the cells with morphological changes.

measuring ROS and  $\text{Ca}^{2+}$  production, and the levels of  $\Delta\Psi_m$ . Results present in Figure 4. CTD increased ROS production at 6–12 h treatment but decreased ROS at 24–48 h (Figure 4(a)). CTD increased  $\text{Ca}^{2+}$  production at 6–48 h treatment (Figure 4(b)); however, decreased the levels of  $\Delta\Psi_m$  at 12–48 h treatment (Figure 4(c)).

Furthermore, U-2 OS cells were also incubated with CTD (0 and 6 μM) for 6, 12, 24 and 48 h and were harvested for measuring caspase-3 and caspase-9 activity. As shown in Figure 5(a), CTD significantly decreased caspase-3 activity at 6–24 h treatment but significantly increased at 48 h in U-2 OS cells. Moreover, CTD significantly decreased caspase-9 activity at 12–24 h treatment but significantly increased at 48 h in U-2 OS cells (Figure 5(b)). Based on these results, we suggest that CTD decreased total viable cells may through ROS,  $\text{Ca}^{2+}$ , mitochondria and caspase-associated apoptosis *in vitro*.

### CTD altered DNA damage, ROS, cell cycle, and apoptosis-associated proteins expression in U-2 OS cells

For further understanding whether alterations of protein expressions were involved in CTD induced DNA damage, ROS production, cell cycle and cell apoptosis in U-2 OS cells. Cells were treated with CTD (6 μM) for 0, 6, 12, 24 and 48 h and then protein expressions were examined by western blotting and results are shown in Figure 6. Results indicated that CTD increased the expression of DNA damage-associated proteins. CTD increased p-ATM at 12–24 h, p-ATR at 6–12 h, DNA-PK at 12 h, and active form of PARP at 12–48 h treatment (Figure 6(a)). For cell cycle assay, CTD increased CHK1, p-p53, and WEE-1 at 6–48 h treatment, CDC25C at 6–24 h, and CDK1 and p21 at 6 h. However, CTD decreased CDC25C at 48 h treatment, CDK1 at 12–48 h, and p21 at 24–48 h (Figure 6(b)) in U-2 OS cells that associated with induced  $G_2/M$  phase arrest.



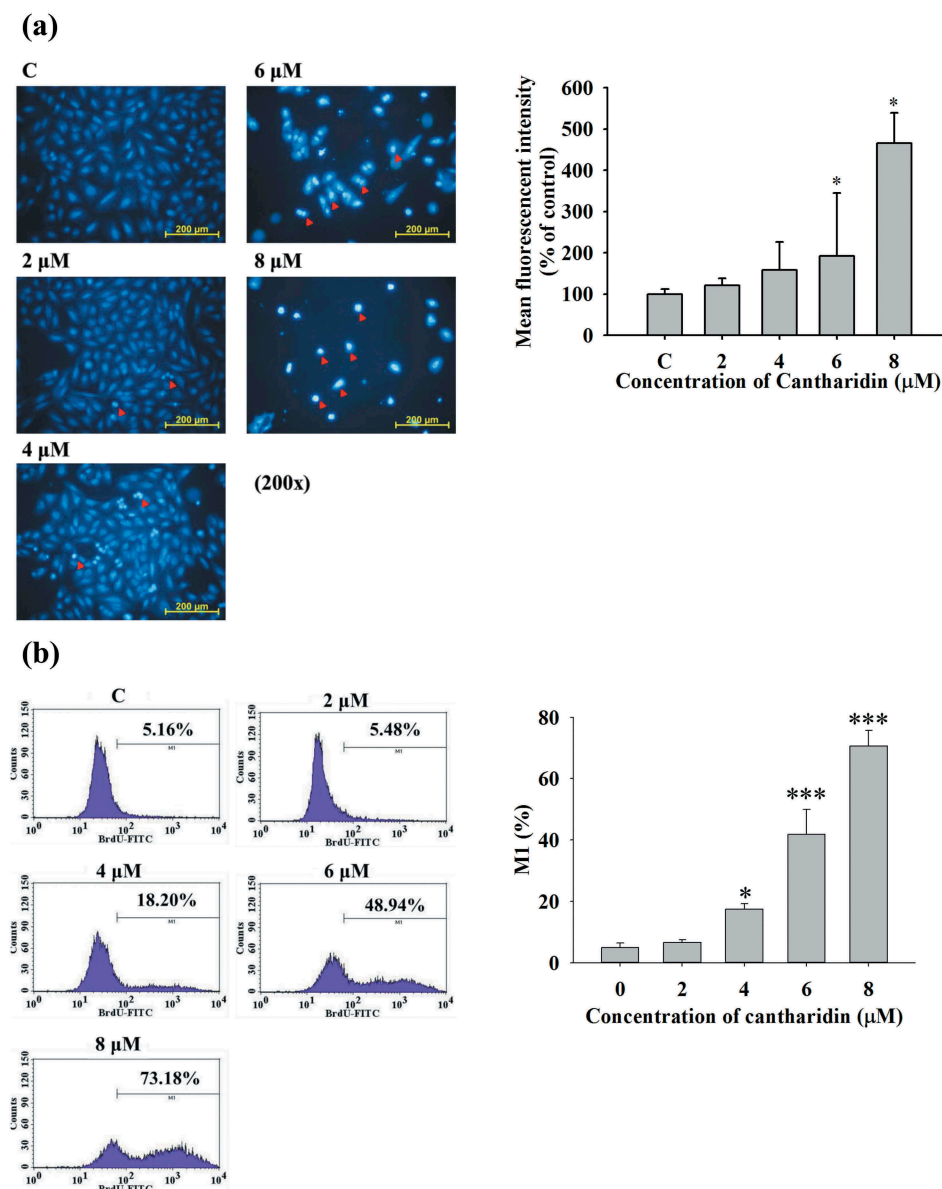


**Figure 2.** CTD induced apoptosis in U-2 OS cells. U-2 OS cells ( $1 \times 10^5$  cells/well) were cultured onto 12-well plate and incubated with CTD (0, 2, 4, 6 and 8  $\mu\text{M}$ ) for 48 h.

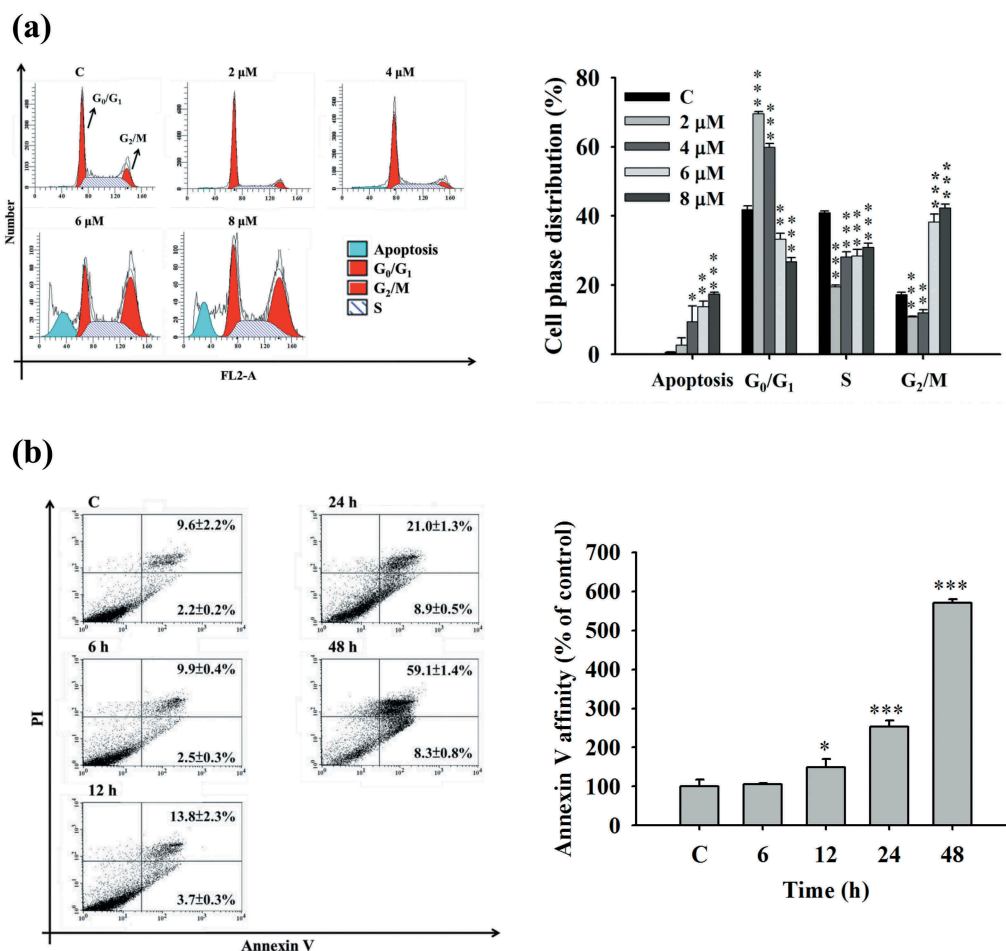
Cells were stained with DAPI solution (2  $\mu\text{g}/\text{mL}$ ), followed by photographed using a fluorescence microscope as described previously (a). Or cells were stained with TUNEL assay kit and analyzed by flow cytometry (b) as described in Materials and Methods. The results were expressed as the mean  $\pm$  standard deviation (SD). \* $p < 0.05$  and \*\*\* $p < 0.001$ , significant difference between CTD-treated groups and the control as analyzed by one-way ANOVA. Arrowheads indicated the cells with morphological changes.

Figure 6C indicates that CTD increased SOD(Cu/Zn), SOD (Mn) and catalase at treated time (6–48 h) that associated with ROS production. Furthermore, CTD increased GADD 153 and GRP78 at 6–48 h, caspase-4 at 6–24 h, and IRE-1 $\alpha$  at 6–12 h treatment (Figure 6(d)) in U-2 OS cells, which related to ER stress. Results showed that CTD increased active form of caspase-3 at 12–48 h, caspase-9 at 12–24 h, and cytochrome c at 6–48 h treatment, however, significantly reduced the levels of XIAP at 6–12 h treatment (Figure 6(e)) which regulated the apoptosis effects. CTD increased Bad, Bax, and Bid at 12–24 h, Endo G at 6–24 h, and AIF at 6–48 h treatment (Figure 6(f)). CTD also increased the expression of Bak at 12 and 48 h treatment. CTD increased Fas, TRAIL, and FADD at 6–48 h treatment and Fas-L at 6–12 h treatment (Figure 6(g)). These

results may suggest that CTD induced cell apoptosis may occur through these receptors in U-2 OS cells.

## Discussion

Numerous studies have demonstrated that CTD present cytotoxic effects on many human cancer cell lines via the cell cycle arrest and the induction of cell apoptosis *in vitro*, however, there is no available information to show CTD induced apoptosis in human osteosarcoma cells. Thus, in the present study, we investigated the effects of CTD on the induction of apoptosis and explored its possible signaling pathways. The results indicated that CTD induced cell morphological changes and decreased total viable cell number in U-2 OS cells in dose-dependently (Figure 1). This is in agreement with



**Figure 3.** CTD induced cell cycle arrest and apoptosis in U-2 OS cells. Cells ( $1 \times 10^5$  cells/well) were cultured in 12-well plate and were incubated with 0, 2, 4, 6 and 8  $\mu\text{M}$  of CTD for 48 h. Cells were isolated and stained with PI and then were analyzed by flow cytometry as described in Materials and Methods (a). Or cells were incubated with 6  $\mu\text{M}$  of CTD for 0, 6, 12, 24 and 48 h and were harvested and resuspended in Annexin V binding buffer, followed incubated with Annexin V-FITC/PI for total apoptotic cell death analysis by flow cytometry as in Materials and Methods (b). The results were expressed as the mean  $\pm$  standard deviation (SD). \* $p < 0.05$ , \*\* $p < 0.01$  and \*\*\* $p < 0.001$ , significant difference between CTD-treated groups and the control as analyzed by one-way ANOVA.

other report showed in TSGH-8301 human bladder carcinoma cells [23]. We further used DAPI and TUNEL staining assay to detect the apoptosis effects of CTD-treated U-2 OS cells, and these results also indicated that CTD induced apoptotic cell death (Figure 2). Both methods (DAPI and TUNEL staining) for examining cell apoptosis are well known; thus, herein, we also used them to confirm CTD induced cell apoptosis in U-2 OS cells.

Apoptosis (a programmed cell death) plays an important process to eliminate redundant and abnormal cells, however, it also associated with cancer development [31]. In carcinoma, cells are deregulated cell death (apoptosis) and restoring apoptosis has been recognized to be one of the most studied processes in cancer therapy. Herein, we also used PI staining for sub-G<sub>1</sub> phase and cell cycle distribution examination and used Annexin-V/PI double staining for examining apoptotic cell death in U-2 OS cells after exposed to various concentrations of CTD and results indicated that CTD induced sub-G<sub>1</sub>

accumulation, G<sub>2</sub>/M phase arrest, and cell apoptosis in U-2 OS cells (Figure 3). These findings are in agreement with other reports in CTD treated breast [32] and gastric [33] cancer cells.

Therefore, we further investigated the molecular mechanism of CTD induced apoptosis in U-2 OS cells. We used western blotting to show CTD significantly increased CHK1, p-p53, and WEE1 but reduced CDC25C and CDK1 and p21 expressions (Figure 6(b)) in U-2 OS cells that associated with induced G<sub>2</sub>/M phase arrest. DNA damage is associated with p53. Thus, results also showed that CTD significantly increased DNA damage-associated proteins (p-ATM, p-ATR, and DNA-PKcs) at 6–12 h treatments and significantly increased active form of PARP (Figure 6(a)) at 12–48 h. PARP is one of the targets of caspase and it is also associated with apoptosis. After induction of DNA damage, PARP will auto-modify and recruit repair factors to the DNA damage sites [34,35]. More interesting is that in human patients and animal models have

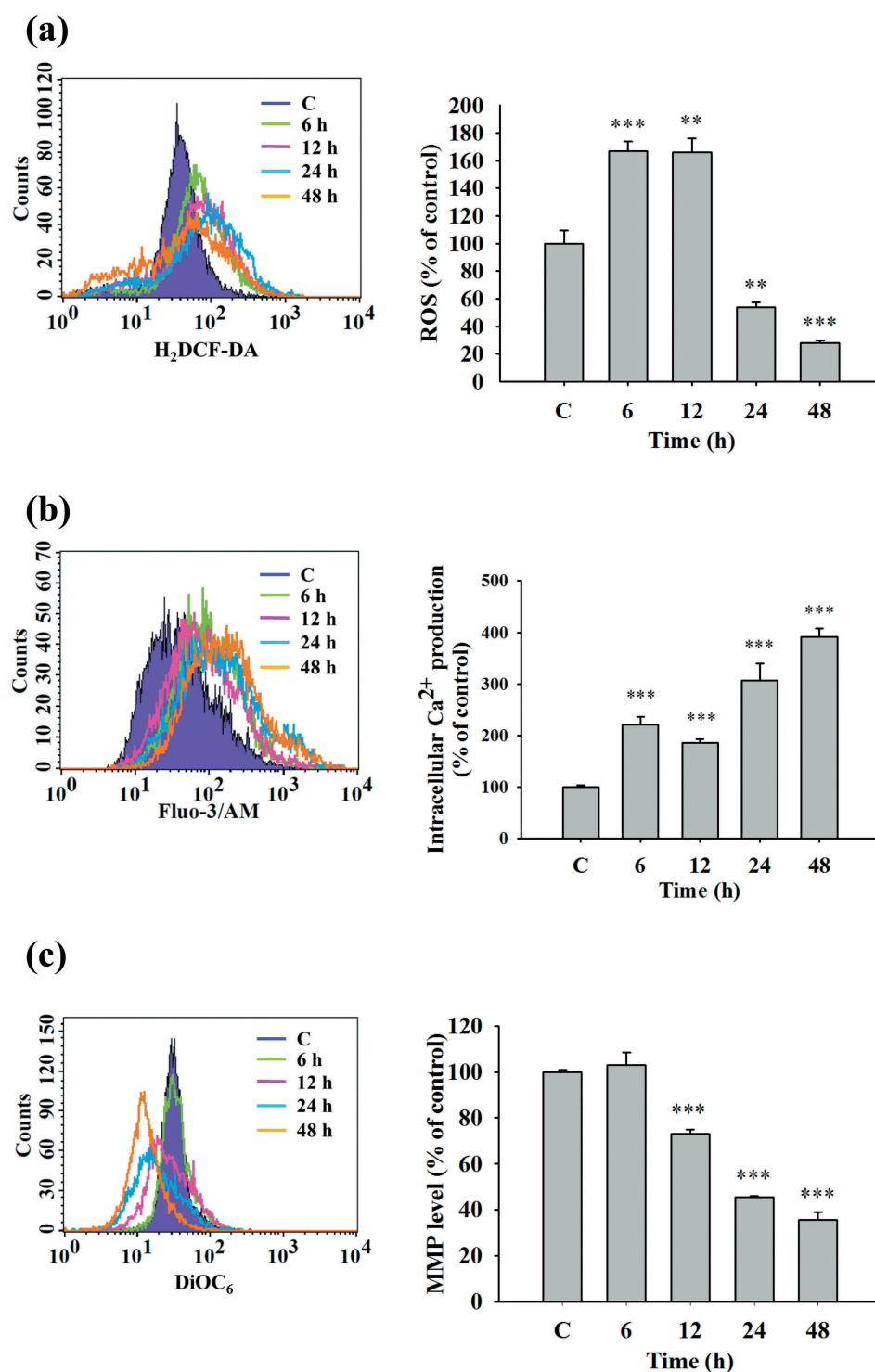


**Figure 4.** CTD induced reactive oxygen species (ROS) and Ca<sup>2+</sup> productions and decreased the levels of mitochondrial membrane potential ( $\Delta\Psi$ m) in U-2 OS cells. Cells were incubated 6  $\mu$ M of CTD for 0, 6, 12, 24 and 48 h for measuring ROS (a) and Ca<sup>2+</sup> (b) production and the levels of  $\Delta\Psi$ m (c) as described in Materials and Methods. The results were expressed as the mean  $\pm$  standard deviation (SD). \* $p$  < 0.05, \*\* $p$  < 0.01 and \*\*\* $p$  < 0.001, significant difference between CTD-treated groups and the control as analyzed by one-way ANOVA.

shown that *p53* and *Rb* gene/pathway dysregulation is central to the formation of osteosarcoma [36–38]. These observations suggested the molecular mechanisms of DNA damage and G<sub>2</sub>/M arrest were involved in U-2 OS cells after exposed to CTD.

Apoptosis is regulated by two principal pathways: the death receptor-mediated (extrinsic) and the mitochondrial-dependent (intrinsic) pathways [11]. The

death receptor-mediated (extrinsic) is triggered by Fas-FasL interaction, FADD recruitment, and caspase-8 activation for either through caspase-3 to induce apoptosis [39] or signaling to mitochondria for the mitochondrial-dependent (intrinsic) pathway. Activation of caspase-4 by ER stress also leads to mitochondrial-dependent (intrinsic) pathway [40]. In this study, we examined the factors involved in

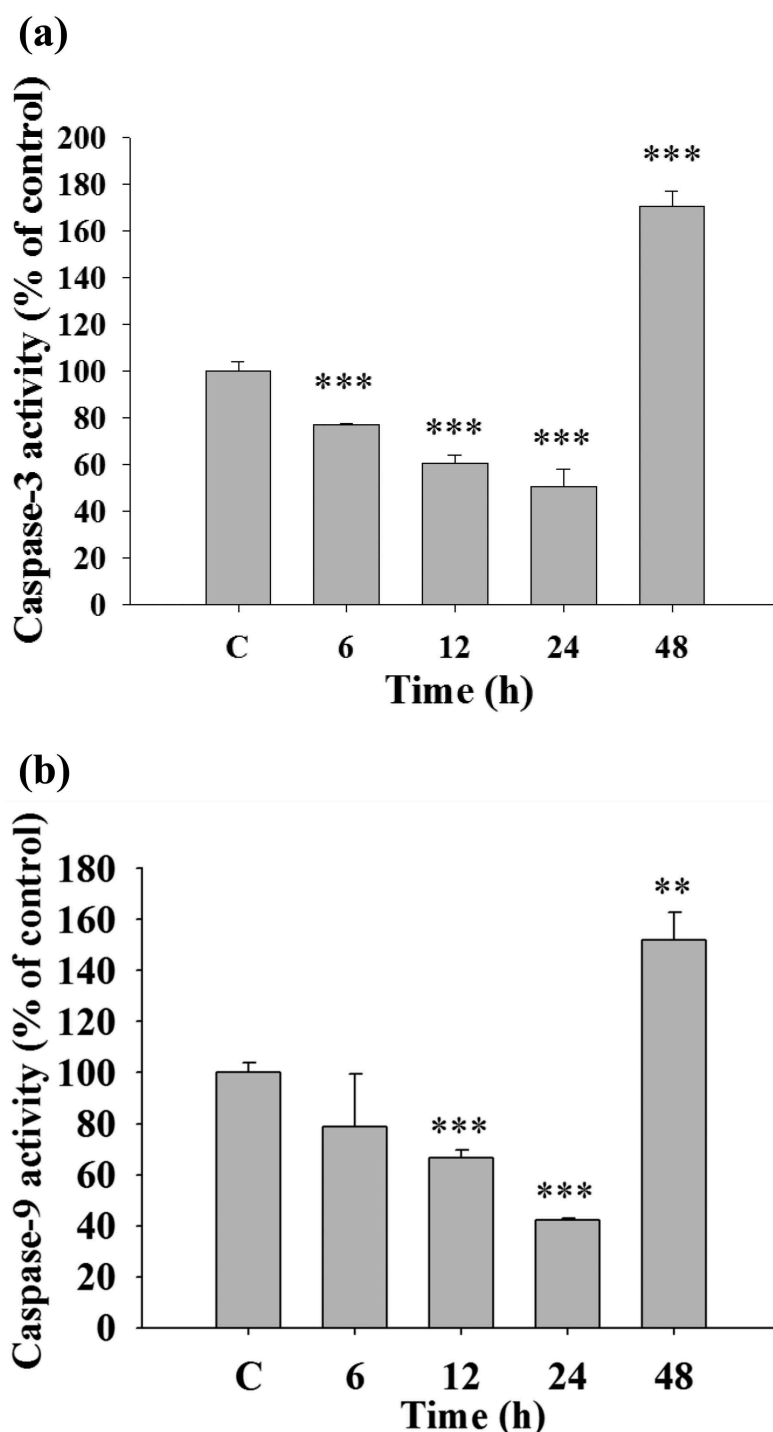


**Figure 5.** CTD affected the activities of caspase-3 and -9 in U-2 OS cells.

Cells were treated with 6  $\mu\text{M}$  of CTD for 0, 6, 12, 24 and 48 h and cells were collected to measure the activities of caspase-3 (a) and -9 (b) by flow cytometry as described in Materials and Methods. The results were expressed as the mean  $\pm$  standard deviation (SD). \* $p < 0.05$ , \*\* $p < 0.01$  and \*\*\* $p < 0.001$ , significant difference between CTD-treated groups and the control as analyzed by one-way ANOVA.

intrinsic pathway, ROS and  $\text{Ca}^{2+}$  productions, the levels of mitochondrial membrane potential ( $\Delta\Psi\text{m}$ ), and caspase activities in U-2 OS cells after exposed to 6  $\mu\text{M}$  CTD for various periods. Results indicated that CTD increased ROS and  $\text{Ca}^{2+}$  productions and decreased the levels of  $\Delta\Psi\text{m}$  and increase caspase-3 and -9 activities (Figures 4 and 5). These findings are in agreement with earlier reports from human melanoma cells [41] and lung cancer cells [42]. The mitochondrial-dependent (intrinsic) pathway is initiated

with the loss of membrane integrity and mitochondrial depolarization that have been recognized to be regulated by members of the Bcl-2 protein family for triggering the release of cytochrome *c* and activating caspase-3 as an effector in cell apoptosis [11].

Apoptosis usually was induced by ROS and ER stress. The generation of ROS in cells exists in equilibrium with a wide variety of antioxidant defenses to scavenge free radicals (superoxide and hydroxyl radicals) or nonradicals (hydrogen peroxide;  $\text{H}_2\text{O}_2$ )



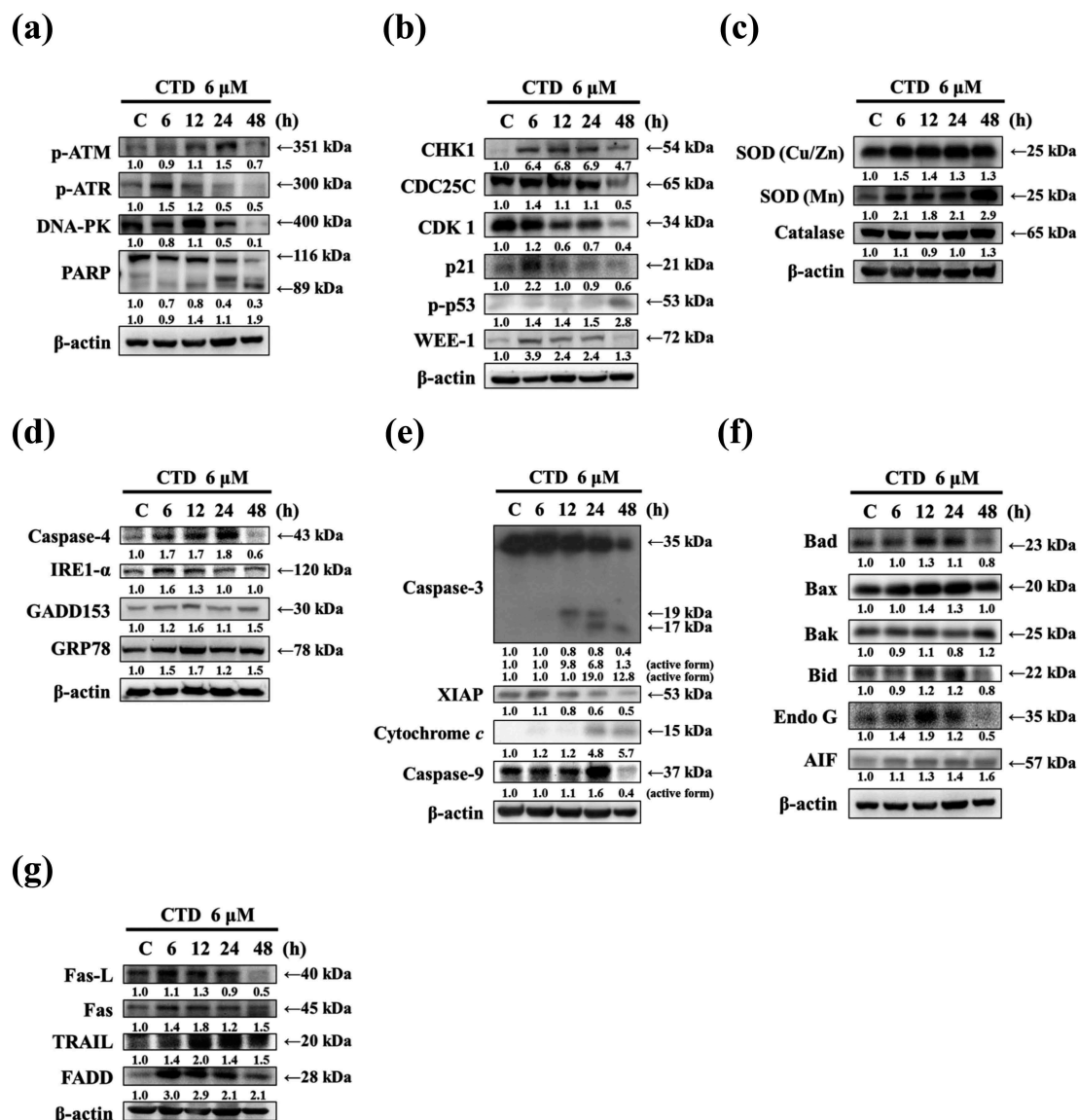


**Figure 6.** CTD induced DNA damage, cell cycle distribution, ROS production, ER stress and apoptosis associated protein expression in U-2 OS cells.

Cells were treated with CTD (6 μM) for 0, 6, 12, 24 and 48 h and then proteins were measured and quantitated with Western blotting as described in Materials and Methods. (a): p-ATM, p-ATR, DNA-PK and PARP; (b): CHK1, CDC25C, CDK1, p21, p-p53 and WEE1; (c): SOD (Cu/Zn), SOD (Mn) and Catalase; (d): caspase-4, IRE1-α, GADD153 and GRP78; (e): caspase-3, XIAP, cytochrome c and caspase-9; (f): Bad, Bax, Bak, Bid, AIF, and Endo G; (g): Fas-L, Fas, TRAIL, and FADD.

[43]. The antioxidant reaction includes enzymatic scavengers [superoxide dismutases (SOD), catalase, glutathione peroxidase, and peroxiredoxins] and as non-enzymatic scavengers (glutathione; GSH) [44]. CTD induced ROS production in time-dependently (Figure 4(a)) and results of western blotting also indicated that CTD increased SOD (Cu/Zn), SOD (Mn) and catalase expression (Figure 6(c)) that associated with ROS production [45].

Furthermore, CTD increased the expressions of GADD153, GRP78, and IRE-1α and also increase that of caspase-4 at 6–24 h treatment (Figure 6(d)) that are also the hallmarks of ER stress [46]. The endoplasmic reticulum (ER) is a major site of protein synthesis and modification, protein folding, and  $\text{Ca}^{2+}$  storage compartments. ER stress will be induced by the accumulation of unfolded or misfolded proteins

within the ER lumen and resulted in  $\text{Ca}^{2+}$  released into the cytoplasm followed by activation of kinases or proteases leading to DNA damage and apoptosis [47,48]. ER also regulates apoptosis by transferring  $\text{Ca}^{2+}$  to mitochondria and triggered cell death [49].

In addition, CTD increased the active form of caspase-3 and -9, and cytochrome c (Figure 6(e)) that associated with decreased of  $\Delta\Psi\text{m}$  [50], furthermore, CTD also increased the pro-apoptotic proteins such as Bad, Bax, and Bak (Figure 6(f)) and increased Endo G and AIF (Figure 6(f)) in U-2 OS cells. It is well known that Bcl-2 family such as Bad, Bax, and Bak are associated with cell apoptosis [51], and Endo G and AIF are also involved in cell apoptosis both can directly enter to nuclei for causing apoptosis [16]. Furthermore, CTD increased the levels of Fas, TRAIL, and FADD at 6–48 h treatment and that of

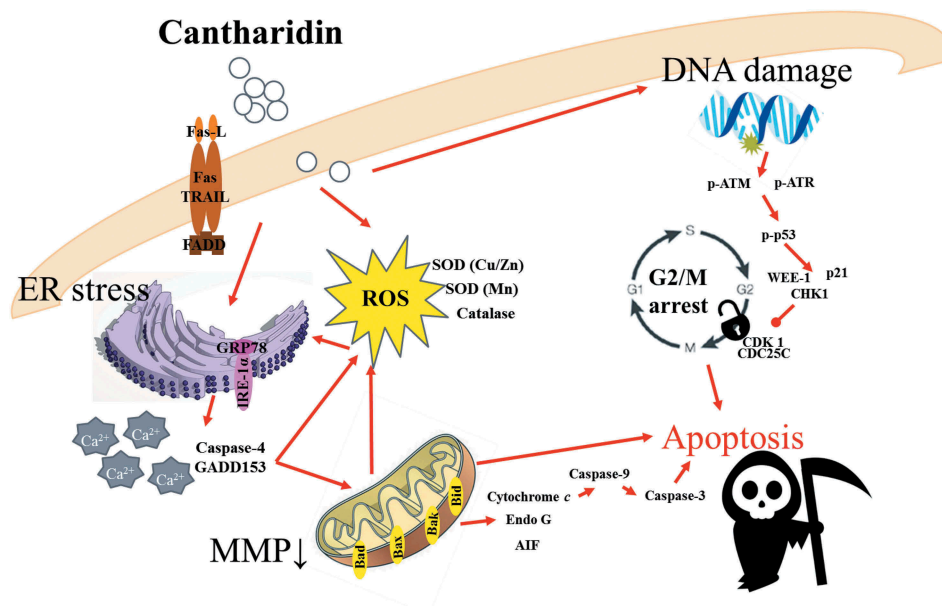


**Figure 7.** The possible signaling pathways for CTD induced apoptosis in U-2 OS human osteosarcoma cancer cells.

Fas-L at 6–12 h (Figure 6(g)). The extrinsic pathways may mediate several receptors such as Fas, TRAIL, DR5, and DR4, which are involved in the extrinsic pathways and followed by activating caspase-8 and either to activate caspase-3 for apoptosis induction or to trigger dysfunction of mitochondria for inducing the intrinsic cell apoptotic pathways [52,53]. Based on these observations, we may suggest that CTD induced cell apoptosis through the death receptors in U-2 OS cells *in vitro*.

In summary, CTD induced cytotoxic effects on human osteosarcoma U-2 OS cells through induced G<sub>2</sub>/M phase arrest and apoptosis *in vitro*. Cell apoptosis also was confirmed by Annexin-V/PI double staining and associated protein expressions by western blotting, and the possible signaling pathway were showing in Figure 7. CTD triggered cell apoptosis may occur via Fas, TRAIL receptor for the extrinsic pathway and mitochondria-dependent intrinsic pathway in U-2 OS cells.

### Author contributions

Study conception and design: C.C.C., Y.P.H. and J.G.C.; Acquisition of data: C.C.C., F.S.C., S.F.P. and W.W.H.; Analysis and interpretation of data: C.C.C., C.H.T., F.J.T., C.Y.H., C.H.T., J.S.Y. and Y.M.H.; Drafting of manuscript: Y.P.H. and J.G.C.; Critical revision: F.S.C., S.F.P., Y.P.H. and J.G.C. All authors discussed the results and commented on the manuscript.

### Disclosure statement

No potential conflict of interest was reported by the authors.

### Funding

This work was supported from a research grant from Ministry of Science and Technology, Taipei, Taiwan [104-2815-C-039-025-B] and from China Medical University, Taichung, Taiwan [CMU106-ASIA-01]. Experiments and data analysis were performed in part through the use of the Medical Research Core Facilities Center, Office of Research & Development at China Medical University, Taichung, Taiwan.

### ORCID

Yuan-Man Hsu  <http://orcid.org/0000-0002-4575-7475>

### References

- [1] Bielack SS, Kempf-Bielack B, Delling G, et al. Prognostic factors in high-grade osteosarcoma of the extremities or trunk: an analysis of 1,702 patients treated on neoadjuvant cooperative osteosarcoma study group protocols. *J Clin Oncol*. 2002;20:776–790.
- [2] Mirabello L, Troisi RJ, Savage SA. Osteosarcoma incidence and survival rates from 1973 to 2004: data from the surveillance, epidemiology, and end results program. *Cancer*. 2009;115:1531–1543.
- [3] Jemal A, Siegel R, Ward E, et al. Cancer statistics, 2008. *CA Cancer J Clin*. 2008;58:71–96.
- [4] Wang Y, Chen J, Zhang D, et al. Tumoricidal effects of a selenium (Se)-polysaccharide from Ziyang green tea on human osteosarcoma U-2 OS cells. *Carbohydr Polym*. 2013;98:1186–1190.
- [5] Ferrari S, Smeland S, Mercuri M, et al. Neoadjuvant chemotherapy with high-dose Ifosfamide, high-dose methotrexate, cisplatin, and doxorubicin for patients with localized osteosarcoma of the extremity: a joint study by the Italian and Scandinavian Sarcoma Groups. *J Clin Oncol*. 2005;23:8845–8852.
- [6] Marina N, Gebhardt M, Teot L, et al. Biology and therapeutic advances for pediatric osteosarcoma. *Oncologist*. 2004;9:422–441.

- [7] Yang J, Zhang W. New molecular insights into osteosarcoma targeted therapy. *Curr Opin Oncol.* **2013**;25:398–406.
- [8] Ottaviani G, Jaffe N. The epidemiology of osteosarcoma. *Cancer Treat Res.* **2009**;152:3–13.
- [9] Han G, Wang Y, Bi W, et al. MicroRNA-124 functions as a tumor suppressor and indicates prognosis in human osteosarcoma. *Exp Ther Med.* **2015**;9:679–684.
- [10] Elmore S. Apoptosis: a review of programmed cell death. *Toxicol Pathol.* **2007**;35:495–516.
- [11] Cui L, Bu W, Song J, et al. Apoptosis induction by alantolactone in breast cancer MDA-MB-231 cells through reactive oxygen species-mediated mitochondrion-dependent pathway. *Arch Pharm Res.* **2018**;41:299–313.
- [12] Muzio M, Chinnaiyan AM, Kischkel FC, et al. FLICE, a novel FADD-homologous ICE/CED-3-like protease, is recruited to the CD95 (Fas/APO-1) death-inducing signaling complex. *Cell.* **1996**;85:817–827.
- [13] Martin DA, Siegel RM, Zheng L, et al. Membrane oligomerization and cleavage activates the caspase-8 (FLICE/MACHalpha1) death signal. *J Biol Chem.* **1998**;273:4345–4349.
- [14] Brauns SC, Dealtry G, Milne P, et al. Caspase-3 activation and induction of PARP cleavage by cyclic dipeptide cyclo(Phe-Pro) in HT-29 cells. *Anticancer Res.* **2005**;25:4197–4202.
- [15] Arnoult D, Gaume B, Karbowski M, et al. Mitochondrial release of AIF and EndoG requires caspase activation downstream of Bax/Bak-mediated permeabilization. *Embo J.* **2003**;22:4385–4399.
- [16] Liu KC, Huang YT, Wu PP, et al. The roles of AIF and Endo G in the apoptotic effects of benzyl isothiocyanate on DU 145 human prostate cancer cells *via* the mitochondrial signaling pathway. *Int J Oncol.* **2011**;38:787–796.
- [17] Breckenridge DG, Germain M, Mathai JP, et al. Regulation of apoptosis by endoplasmic reticulum pathways. *Oncogene.* **2003**;22:8608–8618.
- [18] Bravo-Sagua R, Rodriguez AE, Kuzmich J, et al. Cell death and survival through the endoplasmic reticulum-mitochondrial axis. *Curr Mol Med.* **2013**;13:317–329.
- [19] Nickolls LC, Teare D. Poisoning by cantharidin. *Br Med J.* **1954**;2:1384–1386.
- [20] Huh JE, Kang KS, Chae C, et al. Roles of p38 and JNK mitogen-activated protein kinase pathways during cantharidin-induced apoptosis in U937 cells. *Biochem Pharmacol.* **2004**;67:1811–1818.
- [21] Huan SK, Lee HH, Liu DZ, et al. Cantharidin-induced cytotoxicity and cyclooxygenase 2 expression in human bladder carcinoma cell line. *Toxicology.* **2006**;223:136–143.
- [22] Sagawa M, Nakazato T, Uchida H, et al. Cantharidin induces apoptosis of human multiple myeloma cells *via* inhibition of the JAK/STAT pathway. *Cancer Sci.* **2008**;99:1820–1826.
- [23] Kuo JH, Chu YL, Yang JS, et al. Cantharidin induces apoptosis in human bladder cancer TSGH 8301 cells through mitochondria-dependent signal pathways. *Int J Oncol.* **2010**;37:1243–1250.
- [24] Huang WW, Ko SW, Tsai HY, et al. Cantharidin induces G2/M phase arrest and apoptosis in human colorectal cancer colo 205 cells through inhibition of CDK1 activity and caspase-dependent signaling pathways. *Int J Oncol.* **2011**;38:1067–1073.
- [25] Li CC, Yu FS, Fan MJ, et al. Anticancer effects of cantharidin in A431 human skin cancer (Epidermoid carcinoma) cells *in vitro* and *in vivo*. *Environ Toxicol.* **2017**;32:723–738.
- [26] Hsia TC, Yu CC, Hsiao YT, et al. Cantharidin impairs cell migration and invasion of human lung cancer NCI-H460 cells *via* UPA and MAPK signaling pathways. *Anticancer Res.* **2016**;36:5989–5997.
- [27] Chueh FS, Chen YY, Huang AC, et al. Bufalin-inhibited migration and invasion in human osteosarcoma U-2 OS cells is carried out by suppression of the matrix metalloproteinase-2, ERK, and JNK signaling pathways. *Environ Toxicol.* **2014**;29:21–29.
- [28] Lu CC, Yang JS, Chiang JH, et al. Novel quinazolinone MJ-29 triggers endoplasmic reticulum stress and intrinsic apoptosis in murine leukemia WEHI-3 cells and inhibits leukemic mice. *PLoS One.* **2012**;7:e36831.
- [29] Lee MR, Lin C, Lu CC, et al. YC-1 induces G0/G1 phase arrest and mitochondria-dependent apoptosis in cisplatin-resistant human oral cancer CAR cells. *Biomedicine (Taipei).* **2017**;7:12.
- [30] Lin M-C, Tsai S-Y, Wang F-Y, et al. Leptin induces cell invasion and the upregulation of matrilysin in human colon cancer cells. *Biomedicine (Taipei).* **2013**;3:174–180.
- [31] Ksiezakowska-Lakoma K, Zyla M, Wilczynski JR. Mitochondrial dysfunction in cancer. *Prz Menopauzalny.* **2014**;13:136–144.
- [32] Gong FR, Wu MY, Shen M, et al. PP2A inhibitors arrest G2/M transition through JNK/Sp1-dependent down-regulation of CDK1 and autophagy-dependent up-regulation of p21. *Oncotarget.* **2015**;6:18469–18483.
- [33] Zhang C, Chen Z, Zhou X, et al. Cantharidin induces G2/M phase arrest and apoptosis in human gastric cancer SGC-7901 and BGC-823 cells. *Oncol Lett.* **2014**;8:2721–2726.
- [34] Lucarini L, Durante M, Lanzi C, et al. HYDAMTIQ, a selective PARP-1 inhibitor, improves bleomycin-induced lung fibrosis by dampening the TGF-beta/SMAD signalling pathway. *J Cell Mol Med.* **2017**;21:324–335.
- [35] Schuhwerk H, Atteya R, Siniuk K, et al. PARPping for balance in the homeostasis of poly(ADP-ribosylation). *Semin Cell Dev Biol.* **2017**;63:81–91.
- [36] Gorlick R, Anderson P, Andrulis I, et al. Biology of childhood osteogenic sarcoma and potential targets for therapeutic development: meeting summary. *Clin Cancer Res.* **2003**;9:5442–5453.
- [37] Chou AJ, Geller DS, Gorlick R. Therapy for osteosarcoma: where do we go from here? *Paediatr Drugs.* **2008**;10:315–327.
- [38] O'Day K, Gorlick R. Novel therapeutic agents for osteosarcoma. *Expert Rev Anticancer Ther.* **2009**;9:511–523.
- [39] Ashkenazi A, Dixit VM. Death receptors: signaling and modulation. *Science.* **1998**;281:1305–1308.
- [40] Hitomi J, Katayama T, Eguchi Y, et al. Involvement of caspase-4 in endoplasmic reticulum stress-induced apoptosis and Abeta-induced cell death. *J Cell Biol.* **2004**;165:347–356.
- [41] Hsiao YP, Tsai CH, Wu PP, et al. Cantharidin induces G2/M phase arrest by inhibition of Cdc25c and Cyclin A and triggers apoptosis through reactive oxygen species and the mitochondriadependent pathways of A375.S2 human melanoma cells. *Int J Oncol.* **2014**;45:2393–2402.

- [42] Hsia TC, Yu CC, Hsu SC, et al. Cantharidin induces apoptosis of H460 human lung cancer cells through mitochondria-dependent pathways. *Int J Oncol.* [2014](#);45:245–254.
- [43] Tudek B, Winczura A, Janik J, et al. Involvement of oxidatively damaged DNA and repair in cancer development and aging. *Am J Transl Res.* [2010](#);2:254–284.
- [44] Halliwell B. Free radicals and antioxidants - quo vadis? *Trends Pharmacol Sci.* [2011](#);32:125–130.
- [45] Ho J C-M, Zheng S, Comhair SA, et al. Differential expression of manganese superoxide dismutase and catalase in lung cancer. *Cancer Res.* [2001](#);61:8578–8585.
- [46] Avril T, Vauleon E, Chevet E. Endoplasmic reticulum stress signaling and chemotherapy resistance in solid cancers. *Oncogenesis.* [2017](#);6:e373.
- [47] Wu Y, Zhang H, Dong Y, et al. Endoplasmic reticulum stress signal mediators are targets of selenium action. *Cancer Res.* [2005](#);65:9073–9079.
- [48] Han J, Back SH, Hur J, et al. ER-stress-induced transcriptional regulation increases protein synthesis leading to cell death. *Nat Cell Biol.* [2013](#);15:481–490.
- [49] Ron D, Walter P. Signal integration in the endoplasmic reticulum unfolded protein response. *Nat Rev Mol Cell Biol.* [2007](#);8:519–529.
- [50] Lee JC, Su CL, Chen LL, et al. Formosanin C-induced apoptosis requires activation of caspase-2 and change of mitochondrial membrane potential. *Cancer Sci.* [2009](#);100:503–513.
- [51] Dewson G, Kluck RM. Mechanisms by which Bak and Bax permeabilise mitochondria during apoptosis. *J Cell Sci.* [2009](#);122:2801–2808.
- [52] Jin Z, El-Deiry WS. Overview of cell death signaling pathways. *Cancer Biol Ther.* [2005](#);4:139–163.
- [53] Jeong SY, Seol DW. The role of mitochondria in apoptosis. *BMB Rep.* [2008](#);41:11–22.